

# Dynamics in Concentrated Solutions of Poly(methyl methacrylate)/Bis(2-ethylhexyl phthalate)

G. Floudas\*

Max-Planck-Institut für Polymerforschung, Postfach 3148, D-55021 Mainz, Germany

A. Rizos

Department of Chemistry, University of Crete, Heraklion 711 10, Crete, Greece

W. Brown

Department of Physical Chemistry, University of Uppsala, Box 532, 75121 Uppsala, Sweden

K. L. Ngai

Naval Research Laboratory, Washington, D.C. 20375

Received November 15, 1993; Revised Manuscript Received February 28, 1994\*

**ABSTRACT:** Photon correlation spectroscopy (PCS) and dielectric spectroscopy (DS) are employed to study the dynamics of density fluctuations at temperatures above and below the glass transition temperature,  $T_g$ , and the dynamics of concentration fluctuations above  $T_g$  in concentrated solutions of poly(methyl methacrylate)/bis(2-ethylhexyl phthalate) (PMMA/DOP). The PCS measurements covered the temperature range between 252 and 373 K, and the DS measurements were made between 200 and 398 K and in the frequency range between  $10^{-2}$  and  $10^5$  Hz. Above  $T_g$  the polarized PCS correlation functions contain contributions from both density and concentration fluctuations for a range of temperatures. The concentration fluctuations are characterized by a relatively narrow distribution of relaxation times compared to the density fluctuations and display the usual  $q^2$ -dependence. The dynamics of both processes conform to the Vogel–Fulcher–Tammann equation, and the coupling model of relaxation can explain their different temperature dependences. The  $\alpha$ -relaxation bifurcates into  $\alpha$ - and  $\beta$ -relaxations below  $T_g$  which can be followed respectively by PCS and DS. The additive alters significantly the dynamics of the  $\alpha$ -relaxation and also has a small effect on the dynamics of the  $\beta$ -relaxation which become faster. Increasing plasticizer content enhances the dielectric  $\beta$ -relaxation but weakens the  $\alpha$ -relaxation. At 20% plasticizer content a single, albeit broad, dielectric relaxation exists ( $\beta$ -relaxation) which is due to the concerted motion of the polymer side group with the polar additive. Similarities with the internal plasticization of PMMA are discussed.

## Introduction

It is known that systems suitable for studying the dynamics of density and concentration fluctuations, using photon correlation spectroscopy (PCS), are plasticized polymers ( $C_{\text{polymer}} \geq 0.7$  g/mL) which have sufficient scattering contrast for observing concentration fluctuations. The first such study<sup>1</sup> on the system poly(cyclohexyl methacrylate)/bis(2-ethylhexyl phthalate) (PCHMA/DOP) revealed two clear steps in the polarized correlation functions measured at temperatures above the glass transition temperature  $T_g$ , for a range of temperatures and which originate from “fast” density and “slow” concentration fluctuations. The two processes have different temperature dependences. The density fluctuations due to the segmental ( $\alpha$ -)relaxation scale with the  $T_g$  of the mixtures, while the concentration fluctuations exhibit a weaker temperature dependence with a residual concentration dependence. Recently,<sup>2</sup> the two processes have also been separated with small-angle X-ray scattering from the total intensity and the measured isothermal compressibility. Moreover, a fast diffusive process has been observed in the system poly(methyl methacrylate) (PMMA)/toluene with  $C_{\text{PMMA}} = 0.8$  g/mL at temperatures below  $T_g$ .<sup>3</sup> Other experimental<sup>4,5</sup> and theoretical<sup>6</sup> efforts have been made to emphasize the coupling of the density to the concentration fluctuations.

In this paper, we employ the system poly(methyl methacrylate)/bis(2-ethylhexyl phthalate) (PMMA/DOP), which is miscible at the high polymer concentrations used, in order to study (i) the dynamics of density and concentration fluctuations above  $T_g$  using PCS and (ii) the dynamics of density fluctuations below  $T_g$ , using dielectric spectroscopy (DS). At temperatures above  $T_g$ , we find two well-separated processes: a fast process due to local segmental relaxation and a slow diffusional process due to concentration fluctuations. The coupling model is employed which can explain the temperature dependences of the corresponding relaxation times. Furthermore, we find that the shift factors for density and concentration fluctuations exhibit different temperature dependences which is also predicted by the coupling model.

At lower temperatures, there exists an additional process ( $\beta$ -relaxation) which is the dominant relaxation in the DS studies of bulk and plasticized PMMA as compared to the suppressed  $\beta$ -relaxation of PCHMA.<sup>7</sup> The molecular mechanism of the  $\beta$ -relaxation in PMMA, which has attracted many investigations,<sup>8–11</sup> is not completely understood.<sup>10</sup> It is thought, however, to arise from the hindered rotation of the  $-\text{COOCH}_3$  group about the C–C bond due to interactions with the main-chain methyl groups of the adjacent units. Matrix effects (main-chain motion) also contribute to some extent.<sup>8</sup> Here we study the effect of a polar additive (DOP) on the  $\beta$ -relaxation of PMMA. We find that, with increasing plasticizer concentration, the dielectric  $\beta$ -relaxation increases in strength but the  $\alpha$ -relaxation strength is weakened. As a

\* Abstract published in *Advance ACS Abstracts*, April 1, 1994.

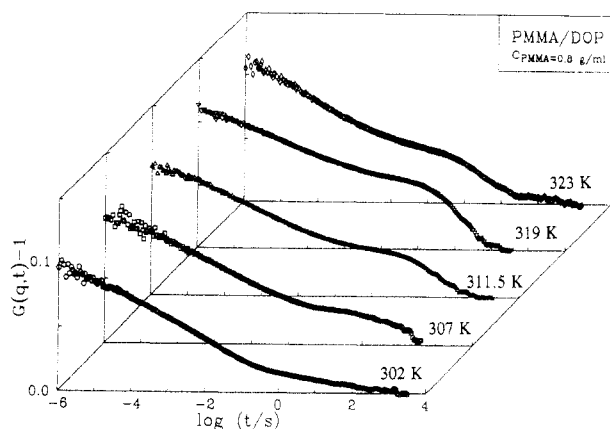


**Figure 1.** Measured correlation functions in the VV geometry for the density and concentration fluctuations in PMMA/DOP at  $C_{\text{PMMA}} = 0.8$  g/mL measured at  $\theta = 90^\circ$  and at the temperatures shown.

result, a single process affects DS at  $C_{\text{PMMA}} = 0.8$  g/mL. We discuss the similarities between internal and external plasticization of PMMA.

### Experimental Section

**Samples.** The PMMA/DOP samples were prepared by thermal polymerization of pure monomer mixtures. The weight-average molecular weight  $M_w$  of PMMA is  $7 \times 10^3$  as determined by gel permeation chromatography (GPC) calibrated by a poly(methyl methacrylate) standard. The glass transition temperature of the bulk polymer is 351 K as determined by differential scanning calorimetry (DSC) at a heating rate of 10 K/min. The  $T_g$ 's for the mixtures with  $C_{\text{PMMA}} = 0.9$  and 0.8 g/mL are 313 and 266 K, respectively.  $T_g$  values for PMMA/DOP mixtures were also reported in ref 12.

**Photon Correlation Spectroscopy (PCS).** The autocorrelation function  $G_{\text{VV}}(q, t)$  of the polarized light scattering intensity was measured at scattering angles of 45, 90, and 145° using an ALV-5000 full digital correlator covering the time range from  $10^{-6}$  to  $10^3$  s. Under homodyne conditions, the desired correlation function is given by

$$G(q, t) = \left[ \frac{G_{\text{VV}}(q, t) - 1}{f} \right]^{1/2} \quad (1)$$

where  $q = (4\pi n/\lambda) \sin(\theta/2)$  is the magnitude of the scattering vector at scattering angle  $\theta$ ,  $n$  is the refractive index of the medium,  $\lambda$  is the wavelength of the incident radiation, and  $f$  is the instrumental factor, calculated by means of a standard. The incident laser beam from an argon ion laser (coherent radiation Model Innova 300) with a  $\lambda = 488$  nm, operating at a single mode with a stabilized power of  $\sim 100$  mW, was used as a light source. Two scattering geometries (VV and VH; V = vertical and H = horizontal) were used by choosing the polarization of the scattered light, whereas the polarization of the incident beam was always perpendicular (V) with respect to the scattering plane. Typical correlation functions in the VV geometry for the plasticized PMMA with 20% DOP are shown in Figure 1. Measurements were made over the  $T$  range 252–373 K.

**Dielectric Spectroscopy (DS).** The real and imaginary parts of the complex dielectric permittivity  $\epsilon^*$  were measured in the frequency range  $10^{-1}$ – $10^5$  Hz with a frequency response analyzer (Solartron Schlumberger 1254) in the temperature range 200–398 K. Samples were kept between two gold-plated stainless steel electrodes, and the sample cell was mounted in a custom-made cryostat. Temperature calibration was accomplished by a jet of temperature-controlled nitrogen gas. Details of the experimental setup can be found elsewhere.<sup>13</sup> The imaginary part  $\epsilon''$  of the dielectric permittivity is plotted in Figure 3 below for the bulk and plasticized PMMA with  $C_{\text{PMMA}} = 0.8$  g/mL.

### Data Analysis

**PCS.** At high  $T$  ( $T > 343$  K), only one relaxation process can be measured in the VV geometry and this is due to

**Table 1.** Relaxation Times for the Density and Concentration Fluctuations in Plasticized PMMA

$T$ (K)	$C_{\text{PMMA}} = 0.9$ g/mL		$C_{\text{PMMA}} = 0.8$ g/mL	
	$-\log \tau_d$	$-\log \tau_c$	$-\log \tau_d$	$-\log \tau_c$
373				2.24
353	4.81	0.17		1.43
343	4.26	−0.91		0.96
338	2.84	−1.79		0.55
333			4.55	0.15
328	0.84	−2.13		
323			3.81	−0.91
319			3.33	−1.49
312			2.67	−2.07
307			2.34	−2.91
302			1.22	
298			0.84	
292			0.61	
288			0.08	
283			−0.51	
277			−0.7	
270			−2.1	

concentration fluctuations (see below). A single Kohlrausch–Williams–Watts (KWW) function was used to fit the correlation functions over this  $T$  range:

$$G(q, t) = \alpha_c \exp[-(t/\tau_c^*(q))^{\beta_c}] \quad (2)$$

treating  $\alpha_c$ ,  $\tau_c^*(q)$ , and  $\beta_c$  as adjustable parameters. At lower  $T$ , in the range  $298 < T < 333$  K the correlation function is clearly bimodal (see Figure 1). The fast process is due to density fluctuations ( $\alpha$ -relaxation), and the slow process is the continuation of the high  $T$  process due to the concentration fluctuations. The two well-separated relaxation processes can be fitted with a double KWW function:

$$G(q, t) = \alpha_d \exp[-(t/\tau_d^*)^{\beta_d}] + \alpha_c \exp[-(t/\tau_c^*)^{\beta_c}] \quad (3)$$

and the shape parameter  $\beta_d$  for the density fluctuations has the values  $0.22 \pm 0.03$  and  $0.2 \pm 0.03$  for the plasticized PMMA with  $C_{\text{PMMA}} = 0.8$  and 0.9 g/mL, respectively. These values indicate an apparent broadening of the distribution for the segmental  $\alpha$ -relaxation in the plasticized polymer compared to that for the bulk polymer ( $\beta_{\text{PMMA}} \sim 0.34$ ). A similar trend of decrease in  $\beta_d$  in going from the bulk to the plasticized polymer was observed before also in PCHMA/DOP.<sup>1</sup> However, the decrease observed in the present system is much larger than that seen in PCHMA/DOP. The shape parameter,  $\beta_c$ , for the concentration fluctuation is equal to  $0.67 \pm 0.15$  and  $0.58 \pm 0.05$  for the samples with  $C_{\text{PMMA}} = 0.8$  and 0.9 g/mL, respectively. As with the system PCHMA/DOP, the  $\beta_c$  values are different than 1 but smaller in the present system as compared to PCHMA/DOP because of the smaller  $M_w$  of PMMA. Table 1 gives the relaxation times for the density and concentration fluctuations for the samples with  $C_{\text{PMMA}} = 0.9$  and 0.8 g/mL.

At even lower  $T$ , in the range  $252 < T < 292$  K, the “slower” process due to concentration fluctuations shifts out of the correlator window, leaving processes due to density fluctuations. In this  $T$  range, broad correlation functions are obtained which cannot be fitted with a single KWW function. A fit to a double KWW function with coupled parameters can be made instead, however. We have chosen, therefore, to analyze the low- $T$  correlation functions by making use of the inverse Laplace transform (ILT) of the time-correlation function:<sup>14</sup>

$$G(q, t) = \int_{-\infty}^{\infty} L(\ln \tau) e^{-t/\tau} d \ln \tau \quad (4)$$

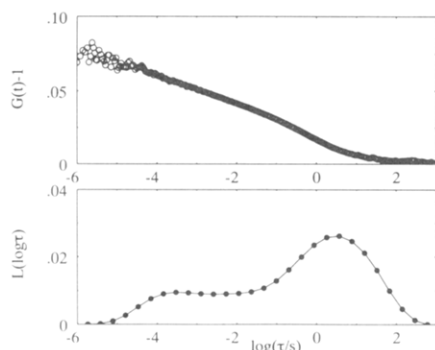


**Figure 2.** Measured correlation function in the VV geometry for the  $C_{\text{PMMA}} = 0.8$  g/mL at  $T = 283$  K. The corresponding retardation time spectrum  $L(\log \tau)$  is also shown.

where  $L(\ln \tau)$  is the distribution of retardation times. Figure 2 shows an experimental time-correlation function, taken at  $T = 283$  K for the  $C_{\text{PMMA}} = 0.8$  g/mL sample together with the result of the ILT. A dual feature is clearly present in  $L(\ln \tau)$ , which is only due to density fluctuations (the process due to concentration fluctuations having moved out of the correlator window). The slower and faster processes in Figure 2 are considered to be due to the segmental ( $\alpha$ -) and  $\beta$ -relaxations, respectively. In order to analyze the faster process at even lower temperature we employ DS which is more sensitive to the  $\beta$ -relaxation because of the strong dipole moment in the side chain of PMMA.

**Dielectric Spectroscopy.** The dielectric data for the bulk and plasticized PMMA (Figure 3) display striking differences. While two processes clearly contribute to the dielectric loss ( $\alpha$ - and  $\beta$ -relaxations) for bulk PMMA, a single broad process is present in the plasticized polymer. As we will discuss later, this process has the features of a  $\beta$ -relaxation at low  $T$  and of an  $\alpha$ -relaxation at higher  $T$ . As a fitting function, we employ the empirical equation of Havriliak–Negami (HN):

$$\epsilon^*(\omega) = \epsilon_{\infty} + \frac{\epsilon_0 - \epsilon_{\infty}}{[1 + (i\omega\tau_{\text{HN}})^{\alpha}]^{\gamma}} \quad (0 < \alpha, \gamma \leq 1) \quad (5)$$

where  $\Delta\epsilon = \epsilon_0 - \epsilon_{\infty}$  is the relaxation strength of the process under investigation and is given by the difference between the low- and high-frequency values of the real part of the dielectric permittivity and  $\tau_{\text{HN}}$  is the characteristic relaxation time. The parameters  $\alpha$  and  $\gamma$  respectively describe the symmetrical and asymmetrical broadening of the distribution of relaxation times. The steep rise at low frequencies (Figure 3) is caused by the electrical conductivity within the sample, which has been fitted by  $\epsilon'' \sim (\sigma_0/\epsilon_f)\omega^{s-1}$ , where  $\sigma_0$  and  $s$  ( $0 \leq s \leq 1$ ) are fitting parameters and  $\epsilon_f$  is the permittivity of free space. Two HN equations were used to describe the bimodal  $\epsilon''(f)$  for the bulk polymer, and a single HN equation was used for the plasticized polymers. Figure 4 shows a fit to the  $\alpha$ - and  $\beta$ -relaxations of PMMA at  $T = 358.6$  K using two HN equations. The fast and slow processes are caused by the  $\beta$ - and  $\alpha$ -relaxations, respectively.

## Results and Discussion

### Density and Concentration Fluctuations above $T_g$ .

The observation of a bimodal distribution with well-separated and yet fully relaxed processes within the time window of the correlator is made possible by use of a correlator encompassing a large dynamic range, making the splicing of correlograms taken over different time ranges unnecessary. The two relaxation processes for the

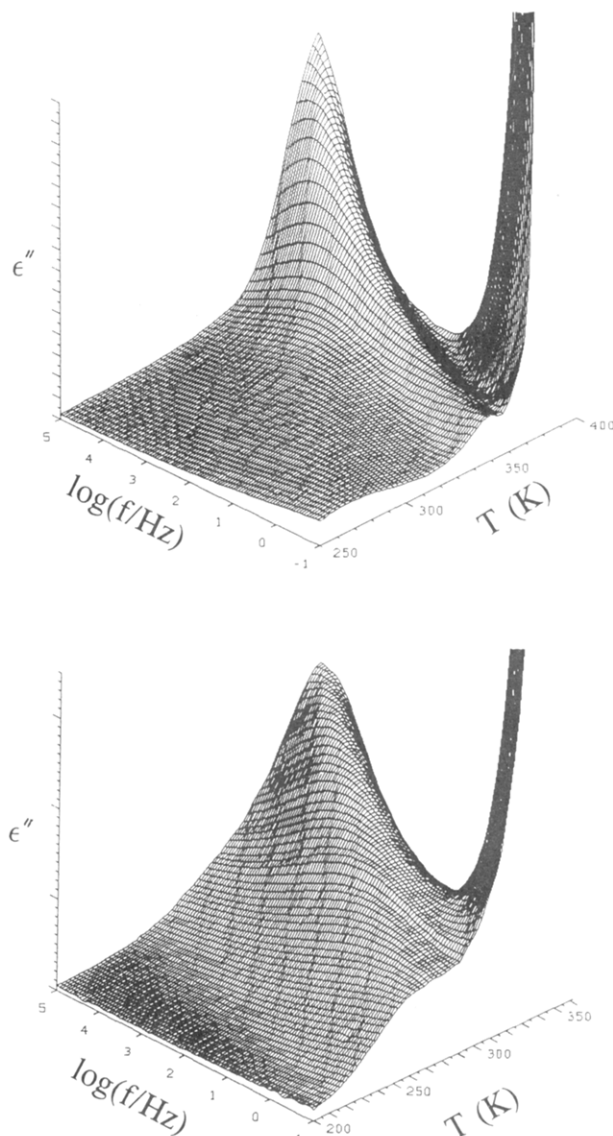


**Figure 3.** Frequency and temperature dependence of the dielectric loss  $\epsilon''$  for bulk PMMA (top) and plasticized PMMA with  $C_{\text{PMMA}} = 0.8$  g/mL (bottom).

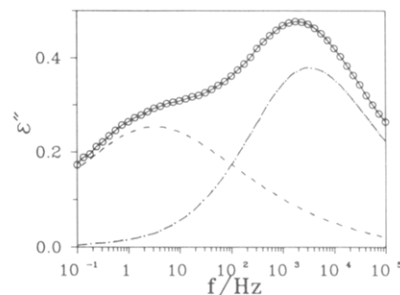


**Figure 4.** Fit of  $\epsilon''$  for the  $\alpha$ - (---) and  $\beta$ -relaxations (---) of bulk PMMA at  $T = 358.6$  K using two Havriliak–Negami equations (eq 5). The solid line is the result of the fit.

plasticized polymer, above  $T_g$  (Figure 1) have been assigned to density and concentration fluctuations. This assignment of the slower process was based on (i) the  $q^2$ -dependence of and (ii) the absence of any depolarized intensity. These results are shown in Figure 5 for the  $C_{\text{PMMA}} = 0.8$  g/mL sample at  $T = 312$  K. The fast process due to density fluctuations contributes in both VV and VH modes, whereas the slow diffusional process is not observed in the VH geometry. Density fluctuations are usually  $q$ -independent for the light scattering  $q$  range, but in

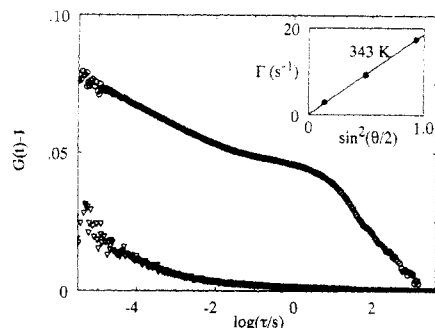


**Figure 5.** Measured correlation functions in the VH geometry (bottom) and in the VV geometry (top) for the  $C_{\text{PMMMA}} = 0.8$  g/mL sample at  $T = 312$  K. The inset shows the  $q^2$ -dependence of the relaxation rate for the concentration fluctuations (at  $T = 343$  K).

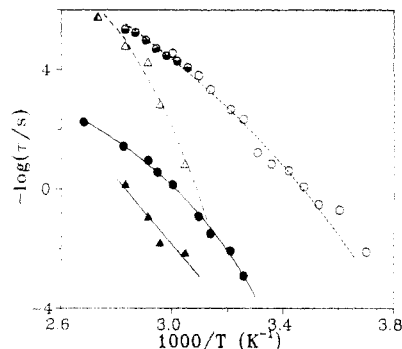


**Figure 6.** Arrhenius plot of the relaxation times for the fast density and slow concentration fluctuations in the  $C_{\text{PMMMA}} = 0.9$  g/mL ( $\Delta, \blacktriangle$ ) and  $0.8$  g/mL ( $\circ, \bullet$ ) obtained from PCS. The half-filled symbols correspond to the data obtained from DS.

quasielastic neutron scattering—where the probing wavelength is near the length scale of the  $\alpha$ -relaxation—the relaxation times depend on  $q$ .<sup>15,16</sup>

The temperature dependence of the dynamics of the density and concentration fluctuations (Figure 6) conform to the Vogel–Fulcher–Tammann (VFT) equation:

$$\log \tau = \log \tau_0 + \frac{B}{T - T_0} \quad (6)$$

where  $\log \tau_0$ ,  $B$ , and  $T_0$  are respectively the intercept, activation energy, and ideal glass transition temperature which is located below the calorimetric  $T_g$  (i.e.,  $T_0 = T_g - c_2$  and  $c_2$  is the WLF coefficient). These parameters for the polymer with  $C_{\text{PMMMA}} = 0.8$  g/mL are  $\log \tau_0 = -14.9 \pm 0.9$ ,  $B_d = 1656 \pm 100$  K, and  $T_0 = 177 \pm 5$  K for  $\tau_d$  of density fluctuations and  $\log \tau_0 = -7.1 \pm 0.5$ ,  $B_c = 610 \pm 40$  K, and  $T_0 = 246 \pm 5$  K for  $\tau_c$  of concentration fluctuations. For the mixture with  $C_{\text{PMMMA}} = 0.9$  g/mL these parameters for  $\tau_d$  of density fluctuations are  $\log \tau_0 = -13.9 \pm 0.9$ ,  $B_d = 757 \pm 60$  K, and  $T_0 = 269 \pm 6$  K. For the concentration fluctuations in this  $C_{\text{PMMMA}} = 0.9$  g/mL sample the relaxation times can only be determined over a narrow temperature range and a fit to the VFT equation cannot be made without introducing large uncertainties. Under this circumstance the best we can do to describe the variation of  $\tau_c$  in a limited temperature range is to use an Arrhenius fit:

$$\log \tau_c = \log \tau_{\infty}^* + \frac{E_{\text{app}}^c}{2.303RT} \quad (7)$$

to the four data points as illustrated in Figure 6. The value obtained for the apparent activation energy  $E_{\text{app}}^c$  is 50.5 kcal/mol. Naturally the validity of eq 7 is limited to

the temperature region in the neighborhood defined by the four data points.

By inspection, Figure 6 clearly shows that for the sample with  $C_{\text{PMMMA}} = 0.9$  g/mL the variation of  $\tau_d$  is considerably more rapid compared with that of  $\tau_c$ . At 269 K the apparent activation energy

$$E_{\text{app}}^d(T=269\text{K}) = \left. \frac{d \ln \tau_d}{d(1/RT)} \right|_{T=269\text{K}} \quad (8)$$

calculated from the VFT fit to  $\tau_d$  has the value of 107 kcal/mol, which is more than a factor of 2 larger than that (50.5 kcal/mol) of  $\tau_c$  at the same temperature. This observation indicates that, had it been possible to carry out measurements at lower temperatures,  $\tau_c$  could eventually approach and become equal to  $\tau_d$ . This spectacular breakdown on thermorheological simplicity in the manner described was first observed by Plazek in viscoelastic measurements of low molecular weight polystyrene<sup>17</sup> and later on poly(methylphenylsiloxane),<sup>18</sup> poly(propylene glycol),<sup>19</sup> and poly(isoprene).<sup>20</sup> In all these previous investigations the effect described was observed only in bulk polymers. Thus our present PCS data from the  $C_{\text{PMMMA}} = 0.9$  g/mL sample together with those already reported for the PCHMA/DOP system show that the same effect occurs also in plasticized polymers. This situation was also observed in a recent study of polystyrene in DOP<sup>21</sup> made over a wide range of temperatures. It was shown there that  $\tau_d$  and  $\tau_c$  merge as anticipated at lower temperatures whereafter  $\tau_c$  follow  $\tau_d$ . It was concluded that the superposition means that the relaxation rate of the concentration fluctuations is determined by the density fluctuations.

An explanation of the difference in the temperature dependences of  $\tau_d$  and  $\tau_c$  has been given by the coupling model.<sup>22</sup> In previous cases where bulk polymers were studied, the coupling parameter,  $n_\alpha$ , for local segmental relaxation was determinable. Since the bulk polymers studied were of low molecular weight with the absence of entanglement coupling, the coupling parameters for the Rouse modes are identically zero. With the coupling parameters of the two viscoelastic mechanisms known, a prediction of the coupling model was able to account for their corresponding observed different temperature dependences quantitatively.<sup>22</sup> PCS on plasticized polymers cannot provide direct measure of  $n_\alpha$  from the shape of the correlation function  $G(q, t)$  because compositional fluctuation has the tendency to broaden the local segmental relaxation response.<sup>23</sup> This is reflected by the fact that in plasticized polymers the stretch exponent,  $\beta_d$ , of the KWW function fit to  $G$  (see eq 3) has become considerably smaller than its value for the unplasticized polymer. Therefore, the quantity  $1 - \beta_d$  should not be identified with the coupling parameter  $n_\alpha$  of local segmental relaxation in plasticized polymers. The latter, from the coupling model standpoint, should be smaller than the coupling parameter of the starting polymer (0.66 for PMMA) and decrease with diluent concentration. The addition of diluent like DOP to PMMA will decrease the capacity for intermolecular cooperativity of the polymer and hence  $n_\alpha$ , the coupling parameter for local segmental relaxation.

For a different reason the difference  $1 - \beta_c$  should not be identified with the coupling parameter  $n_c$  of the diffusion mode, which should be zero in the present case because the  $M_w$  of PMMA is lower than the entanglement molecular weight. The nonzero value of  $1 - \beta_c$  as observed experimentally is caused by the polydispersity of the samples.

According to the coupling model, the temperature and diluent concentration,  $\phi$ , dependences of  $\tau_d$  are derived from those of the primitive friction factor  $\zeta_0(T, \phi)$  by the relation

$$\tau_d \sim (\zeta_0(T, \phi))^{1/[1-n_\alpha(\phi)]} \quad (9)$$

while those of  $\tau_c$  are exactly the same as  $\zeta_0(T, \phi)$ , i.e.

$$\tau_c \sim \zeta_0(T, \phi) \quad (10)$$

From these two relations it follows that the two apparent activation energies given by eqs 7 and 8 are related by

$$E_{app}^d(T = 269K) = \frac{E_{app}^c}{1 - n_\alpha(\phi)} \quad (11)$$

and from which we deduce the value of 0.53 for  $n_\alpha(\phi = 10\%)$ . Although there is considerable uncertainty in this value determined in this way, its magnitude is consistent with the expected decrease of the value of  $n_\alpha$ . Continued addition of diluent will further decrease  $n_\alpha(\phi)$ . As a consequence, from eqs 9–11, the difference between the temperature dependences of  $\tau_d$  and  $\tau_c$  will diminish. This expected trend is consistent with the PCS data of PMMA/DOP at  $\phi = 20\%$ . As can be seen in Figure 6, the different temperature dependences between  $\tau_d$  and  $\tau_c$  are considerably reduced for  $\phi = 20\%$  DOP.

The observations of both  $\tau_d$  and  $\tau_c$  at two concentrations in the PMMA/DOP system offer another application of the coupling model. Conventional wisdom and most known models would suggest that, at constant  $T$ , the two relaxation times would shift by the same amount if the diluent concentration is changed from one value to another. However, the coupling model predicts otherwise. On the one hand,  $\tau_c$  shifts like  $\zeta_0(T, \phi)$  by the amount

$$a_c(\phi) \equiv \frac{\tau_c(T, \phi_1)}{\tau_c(T, \phi_2)} = \frac{\zeta_0(T, \phi_1)}{\zeta_0(T, \phi_2)} \quad (12)$$

but, on the other hand,  $\tau_d$  shifts by

$$a_d(\phi) \equiv \frac{\tau_d(T, \phi_1)}{\tau_d(T, \phi_2)} = \frac{\zeta_0(T, \phi_1)^{1/[1-n_\alpha(\phi_1)]}}{\zeta_0(T, \phi_2)^{1/[1-n_\alpha(\phi_2)]}} \quad (13)$$

If  $\phi_2 > \phi_1$ , from the fact that  $0 < n_\alpha(\phi_2) < n_\alpha(\phi_1)$  and  $\zeta_0(T, \phi_2) < \zeta_0(T, \phi_1)$  it is not difficult to conclude from eqs 12 and 13 that  $a_d(\phi)$  will be much larger than  $a_c(\phi)$ . This is borne out by the experimental data in Figure 6. In the limited temperature range from approximately 320 to 334 K where experimental data for  $\tau_d$  and  $\tau_c$  exist for  $\phi = 10$  and 20%, we have determined for each temperature the two shift factors,  $a_d(\phi)$  and  $a_c(\phi)$ . They are plotted and compared in Figure 7. As predicted by the coupling model,  $a_d(\phi)$  can be made much larger than  $a_c(\phi)$ , particularly at lower temperatures. Other models would expect  $a_d(\phi)$  and  $a_c(\phi)$  to be equal at all temperatures or at least to have temperature dependences that are parallel to each other. Our experimental measurements in PMMA/DOP are in accord with the coupling model.

It is apparent from Figure 6 that the process due to the density fluctuations exhibits different  $T$ -dependences for the two plasticized polymers. This is also indicated by the different activation energies for segmental relaxation. The VFT parameters for the  $\alpha$ -relaxation of bulk PMMA are  $\log \tau_0 = -14.8 \pm 0.9$ ,  $B = 919 \pm 62$  K, and  $T_0 = 290 \pm$

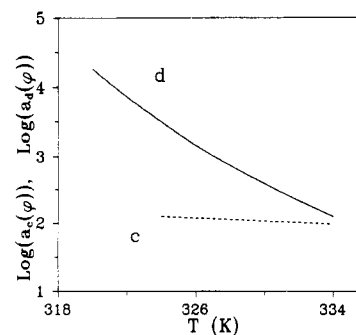


Figure 7. Temperature dependence of the shift factors for density  $a_d(\phi)$  and concentration  $a_c(\phi)$  fluctuations, obtained from the experimental times (Figure 6).

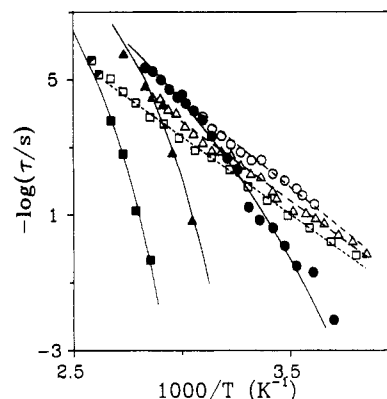
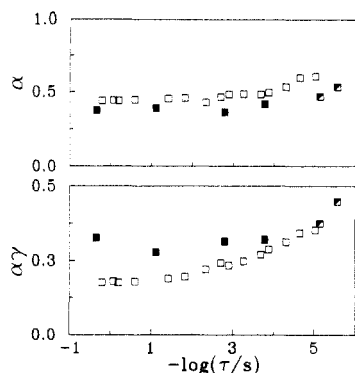


Figure 8. Arrhenius plot of the relaxation times of the  $\alpha$ - (filled symbols) and  $\beta$ -relaxations (open symbols) in bulk ( $\blacksquare, \square$ ) and plasticized PMMA with  $C_{PMMA} = 0.9$  ( $\blacktriangle, \triangle$ ) and 0.8 g/mL ( $\bullet, \circ$ ), respectively, obtained by DS.

3 K ( $c_2 = 61$  K). Consequently, the relaxation times of density fluctuations for the bulk and plasticized polymer with  $C_{PMMA} = 0.9$  g/mL would nearly coincide when plotted vs  $T - T_g$ , but those for the  $C_{PMMA} = 0.8$  g/mL sample will have a different  $T$ -dependence. This observation is at variance with our earlier data for the systems polystyrene/toluene<sup>24</sup> (for  $0.5 < C_{PS} < 1$  g/mL) and PCHMA/DOP<sup>1</sup> ( $0.85 < C_{PCHMA} < 1.0$  g/mL) and will be further discussed below. A plot of the  $\alpha$ -relaxation times of the  $C_{PMMA} = 0.8$  g/mL sample against normalized temperature,  $T_g/T$ , reveals that it is less fragile<sup>25</sup> compared with the sample with  $C_{PMMA} = 0.9$  g/mL. From the empirically established proportionality between fragility (or cooperativity) and coupling parameter<sup>26</sup> we can infer that the coupling parameter  $n_d$  for the  $C_{PMMA} = 0.8$  g/mL sample has been considerably reduced.

**Density Fluctuations below  $T_g$ .** The relaxation process below  $T_g$  is more readily studied by DS because of the strong dipole moment in PMMA. The relaxation times for the  $\beta$ -relaxation of PMMA conform to an Arrhenius equation (eq 7), as shown in Figure 8, with  $\log \tau_0 = -17 \pm 1$  and  $E = 21 \pm 0.5$  kcal/mol in agreement with earlier studies.<sup>8–11</sup> The low- ( $\alpha$ ) and high-frequency ( $\alpha\gamma$ ) slopes of the dielectric loss are shown in Figure 9 for the  $\alpha$ - and  $\beta$ -relaxations and the mixed relaxation at higher  $T$ . The shape parameters  $\alpha$  and  $\gamma$  for the  $\alpha$ -relaxation are  $T$ -independent within the range of our measurements and equal to  $0.39 \pm 0.03$  and  $0.8 \pm 0.06$ , respectively. In contrast, the same parameters for the  $\beta$ -relaxation display a  $T$ -dependence as indicated by the increase of the product  $\alpha\gamma$  at higher frequencies/temperatures. When the two relaxations merge (at  $f \sim 10^5$  Hz), the distribution narrows significantly (Figure 9) and the relaxation strength  $\Delta\epsilon$  of the combined process is doubled (Figure 3). Since  $\Delta\epsilon$  is proportional to the number of dipoles participating in each



**Figure 9.** Frequency dependence of the Havriliak-Negami shape parameters for the bulk PMMA: (●)  $\alpha$ -relaxation, (□)  $\beta$ -relaxation; (■)  $\alpha\beta$ -relaxation.

relaxation by comparing the dielectric strength at a fixed frequency, we can estimate the number of dipoles activated by the  $\beta$ -process as compared to the slower  $\alpha$ -process. Thus, at  $f = 10$  Hz and with the assumption that the same Kirkwood reduction factor affects both relaxations, we find  $(N\mu^2)_\beta/(N\mu^2)_\alpha = T_\beta\Delta\epsilon_\beta/T_\alpha\Delta\epsilon_\alpha = 0.77$ , where  $N$  is the number of monomeric units per unit volume and  $\mu$  is the dipole moment per monomer unit. This indicates that 43% of the total number of dipoles are mobile below  $T_g$ .

In the mixtures with  $C_{\text{PMMA}} = 0.9$  and  $0.8$  g/mL the temperature dependence of the relaxation times (Figure 8) conforms to the Arrhenius equation (eq 7) with parameters  $\log \tau_0^* = -17.8 \pm 1$ ,  $E = 21.5 \pm 0.6$  kcal/mol and  $\log \tau_0^* = -19.9 \pm 1$ ,  $E = 23.7 \pm 1$  kcal/mol, respectively. Although the effect of additive on the activation energy of the  $\beta$ -relaxation is small, it speeds up the relaxation (Figure 8). We can now compare the  $\beta$ -relaxation of PMMA with the low- $T$  relaxation ( $\gamma$ -relaxation) of PCHMA, since we have studied both in the presence of the same additive and over a similar concentration range. The  $\gamma$ -relaxation of PCHMA has<sup>7</sup> (i) an activation energy of  $\sim 11$  kcal/mol, (ii) a distribution of relaxation times of  $\beta_{\text{KWW}} = 0.5$ —as inferred from photon correlation and dielectric spectroscopy—and (iii) an activation energy, a distribution of relaxation times, and absolute values of relaxation times which are insensitive to the additive content. The  $\beta$ -relaxation of PMMA is very different. This relaxation has (i) a higher activation energy ( $\sim 21$  kcal/mol), (ii) a broader distribution of relaxation times (ranging from  $\beta_{\text{KWW}} = 0.19$  at  $T = 263$  K to  $0.37$  at  $T = 374$  K), and (iii) relaxation times which become shorter with increasing DOP content. These experimental results provide sufficient evidence that the  $\beta$ -relaxation in PMMA is intermolecular and cooperative in nature in contrast to the localized  $\gamma$ -relaxation of PCHMA.

The additive has a strong effect not only on the absolute value but also on the distribution of relaxation times. This is shown in Figure 10 for the  $C_{\text{PMMA}} = 0.8$  g/mL sample. The peculiar behavior at  $-\log \tau = 3$  for the high-frequency slope ( $\alpha\gamma$ ) is related to the change in character from a  $\beta$ -relaxation at low  $T$  to an  $\alpha$ -relaxation at higher  $T$ . This is consistent with the good agreement of PCS and DS times above this frequency and with the bifurcation into  $\alpha$ - and  $\beta$ -relaxations at lower  $T$  which influence the PCS and DS spectra, respectively. The polarized PCS correlation functions additionally probe the fast  $\beta$ -relaxation (Figure 2), but in DS the  $\alpha$ - and  $\beta$ -relaxations cannot be seen as separate processes in contrast to bulk PMMA (Figure 3). This is consistent with the increase of the dielectric strength of the  $\beta$ -process at the expense of the  $\alpha$ -process (see below) and explains the absence of the latter process at lower polymer concentrations ( $0 < C_{\text{PMMA}} \leq 0.7$

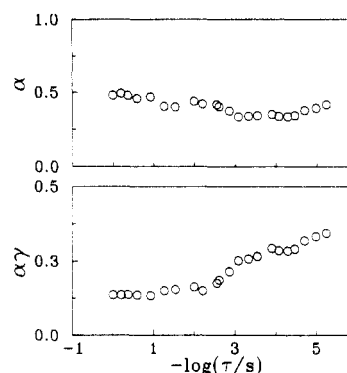


**Figure 10.** Frequency dependence of the Havriliak-Negami shape parameters for the  $C_{\text{PMMA}} = 0.8$  g/mL sample.

g/mL) and also the peculiar  $T$ -dependence of the PCS relaxation times for the  $\alpha$ -relaxation in the  $C_{\text{PMMA}} = 0.8$  g/mL sample at lower  $T$ . Pressure,<sup>27,28</sup> which has a marked effect on the frequency location of the  $\alpha$ -relaxation and a small effect on the  $\beta$ -relaxation, could be used to separate the two processes at  $C_{\text{PMMA}} \leq 0.8$  g/mL.

The experimental findings for the effect of plasticizer on the  $\alpha$ - and  $\beta$ -relaxations of PMMA show similarities with the effect of internal plasticization of PMMA on increasing the length of the alkyl chains. These effects can be summarized as follows: (i) there is a strong shift of the  $\alpha$ -relaxation to lower  $T$  and a much smaller effect on the  $\beta$ -relaxation which, however, also becomes faster;<sup>28</sup> (ii) the strength of the dielectric  $\beta$ -relaxation decreases as a result of the decrease in dipole density;<sup>28,29</sup> (iii) a single relaxation is observed in the case of higher  $n$ -alkyl methacrylates.<sup>28,29</sup> Effects i and iii show striking similarities with the effect of external plasticization of PMMA. However, in contrast to ii the strength of the  $\beta$ -relaxation  $\Delta\epsilon_\beta$  in the PMMA/DOP system is found to increase with plasticizer content. For example, at a frequency of 10 Hz,  $\Delta\epsilon_\beta \approx \Delta\epsilon_\alpha$  for bulk PMMA, but  $\Delta\epsilon_\beta \approx 3\Delta\epsilon_\alpha$  for the sample with  $C_{\text{PMMA}} = 0.9$  g/mL. For higher plasticizer concentrations only a single, albeit broad,  $\beta$ -relaxation is observed which shifts to lower  $T$  (Figure 3). The enhancement of the  $\beta$ -relaxation with increasing plasticizer content is probably caused by the concerted motion of the polymer ester group with the same group in the plasticizer molecules. Dynamic mechanical data<sup>30,31</sup> on plasticized PMMA also show a shift of the  $\beta$ -peak to lower  $T$  and an increased intensity of the dispersion. In particular, for plasticized PMMA with 6% dimethyl phthalate the increase in  $G''$  (at a frequency of 1 Hz) is 11% for the  $\beta$ -relaxation and about 50% for the  $\alpha$ -relaxation.<sup>31</sup> Consequently, the increase in the strength of the dielectric  $\beta$ -peak is much greater than that for the corresponding mechanical peak which is consistent with the picture of the coupled motion between the polymer side group with the polar additive. However, it is puzzling that the motion becomes faster. Additional SAXS measurements which provide the free volume fluctuations through the measured density fluctuations can be used to elucidate this point.

A faster process, associated with the solvent dynamics in their own environment, was not observed for the high  $C_{\text{PMMA}}$  employed in the present study. However, at lower polymer concentrations ( $0 < C_{\text{PMMA}} \leq 0.7$  g/mL) a process which is faster than the  $\beta$ -relaxation and which derives from the solvent dynamics could be observed as with the other concentrated solutions studied earlier.<sup>24,32</sup> This yields the following picture for the DOP mobility in PMMA: At  $C_{\text{PMMA}} \geq 0.8$  g/mL, the plasticizer molecules are evenly dispersed in the polymer matrix and their motions are strongly coupled to the polymer  $\beta$ -relaxation.

With increasing plasticizer concentration more of the plasticizer molecules find themselves in a "plasticizer environment" and exhibit dynamics which are dictated by the fast but modified diluent dynamics. This picture implies a spatially heterogeneous system.

## Conclusions

The simultaneous observation of local segmental dynamics and cooperative diffusion in concentrated polymer solutions by photon correlation spectroscopy is limited to a few systems mainly because of the large separation on the time scales for the two processes. The system PMMA/DOP allowed us to study the dynamics of the fast density and slow concentration fluctuations, above  $T_g$ , over a sufficient temperature range. For the mixture with  $C_{\text{PMMA}} = 0.9 \text{ g/mL}$  we find the familiar picture of  $\tau_d$ , the relaxation times of density fluctuations, to have a more rapid temperature dependence than the corresponding times for concentration fluctuations  $\tau_c$ . For the  $C_{\text{PMMA}} = 0.8 \text{ g/mL}$  system we find, however, the difference between the temperature dependence of  $\tau_d$  and  $\tau_c$  to diminish. This is also reflected in the different temperature dependence of the shift factors for density and concentration fluctuations. Both experimental findings are explained in terms of the coupling model.

At temperatures below  $T_g$ , we have studied the effect of additive on the  $\beta$ -relaxation of PMMA by dielectric spectroscopy. We find that the additive (i) spreads up and (ii) enhances the  $\beta$ -relaxation at the expense of the  $\alpha$ -relaxation. As a consequence, a single, albeit broad, process is observed at  $C_{\text{PMMA}} = 0.8 \text{ g/mL}$ . This behavior implies a concerted motion of the polymer side group with the polar additive at high polymer concentrations. When the present results are combined with measurements on less concentrated solutions, then the emerging picture is of a spatially heterogeneous system.

## References and Notes

- (1) Fytas, G.; Floudas, G.; Ngai, K. L. *Macromolecules* **1990**, *23*, 1104.
- (2) Floudas, G.; Pakula, T.; Fischer, E. W. *Macromolecules* **1994**, *27*, 917.
- (3) Gapinski, J.; Fytas, G.; Floudas, G. *J. Chem. Phys.* **1992**, *96*, 6311.
- (4) Konak, C.; Brown, W. *J. Chem. Phys.* **1993**, *98*, 9014.
- (5) Koch, T.; Strobl, G.; Stühn, B. *Macromolecules* **1993**, *25*, 6255.
- (6) Jäcke, J.; Pieroth, M. *J. Phys.: Condens. Matter* **1990**, *2*, 4963.
- (7) Floudas, G.; Fytas, G.; Fischer, E. W. *Macromolecules* **1991**, *24*, 1955.
- (8) Heijboer, J.; Baas, J. M. A.; van de Graaf, B.; Hoefnagel, M. A. *Polymer* **1987**, *28*, 509.
- (9) Muzeau, E.; Perez, J.; Johari, G. P. *Macromolecules* **1991**, *24*, 4713.
- (10) McCrum, N. G.; Read, B. E.; Williams, G. *Anelastic and Dielectric Effects in Polymeric Solids*; Dover, Inc.: New York, 1991.
- (11) Gomez, J. L.; Diaz, R. *J. Polym. Sci., Polym. Phys. Ed.* **1985**, *23*, 1297.
- (12) Kalachandra, S.; Turner, D. T. *J. Polym. Sci., Polym. Phys. Ed.* **1987**, *25*, 1971.
- (13) Kremer, F.; Boese, D.; Meier, G.; Fischer, E. W. *Progr. Colloid Polym. Sci.* **1989**, *80*, 129.
- (14) Provencher, S. W. *Comput. Phys. Commun.* **1982**, *27*, 229.
- (15) Floudas, G.; Higgins, J. S.; Fytas, G. *J. Chem. Phys.* **1992**, *96*, 7672.
- (16) Colmenero, J.; Alegria, A.; Arbe, A.; Frick, B. *Phys. Rev. Lett.* **1992**, *69*, 478.
- (17) Plazek, D. J.; O'Rourke, V. M. *J. Polym. Sci.* **1971**, *A29*, 209.
- (18) Fytas, G.; Dorfmueller, T.; Chu, B. *J. Polym. Sci., Polym. Phys. Ed.* **1984**, *22*, 1471. Ngai, K. L.; Fytas, G. *J. Polym. Sci., Polym. Phys. Ed.* **1986**, *24*, 1683.
- (19) Ngai, K. L.; Schönhals, A.; Schlosser, E. *Macromolecules* **1992**, *25*, 4915.
- (20) Schönhals, A. *Macromolecules* **1993**, *26*, 1309.
- (21) Brown, W.; Nicolai, T. *Makromol. Chem.*, in press.
- (22) Ngai, K. L.; Plazek, D. J. *J. Polym. Sci., Polym. Phys. Ed.* **1986**, *24*, 619. Ngai, K. L.; Plazek, D. J.; Deo, S. S. *Macromolecules* **1987**, *20*, 3047. Ngai, K. L.; Plazek, D. J.; Bero, C. *Macromolecules*, in press. Plazek, D. J.; Schönhals, A.; Schlosser, E. *J. Chem. Phys.* **1992**, *98*, 6488.
- (23) Fischer, E. W.; Zetsche, A. *Polym. Prepr. (Am. Chem. Soc., Div. Polym. Chem.)* **1992**.
- (24) Floudas, G.; Steffen, W.; Fischer, E. W.; Brown, W. *J. Chem. Phys.* **1993**, *99*, 695.
- (25) Angell, C. A. *J. Non-Cryst. Solids* **1991**, *131-133*, 13.
- (26) Plazek, D. J.; Ngai, K. L. *Macromolecules* **1991**, *24*, 1222. Böhmer, R.; Ngai, K. L.; Angell, C. A.; Plazek, D. J. *J. Chem. Phys.* **1993**, *99*, 4201.
- (27) Williams, G. *Trans. Faraday Soc.* **1964**, *60*, 1548; **1966**, *62*, 2091.
- (28) Sasabe, H.; Saito, S. *J. Polym. Sci., Polym. Phys. Ed.* **1968**, *6*, 1401.
- (29) Ishida, Y.; Yamafuji, K. *Kolloid Z.* **1961**, *177*, 97.
- (30) Heijboer, J. *Int. J. Polym. Mater.* **1977**, *6*, 11.
- (31) Lednicky, F.; Janacek, J. *J. Macromol. Sci., Phys.* **1971**, *B6*, 335.
- (32) Floudas, G.; Fytas, G.; Brown, W. *J. Chem. Phys.* **1992**, *96*, 2164.